Journal of Applied Polymer Science

Measurement and Numerical Prediction of Fiber-Reinforced Thermoplastics' Thermal Conductivity in Injection Molded Parts

Claudio Feliciani, Yoshihiro Takai
Advanced Technology R&D Center, Mitsubishi Electric Corporation, 8-1-1 Tsukaguchi-Honmachi, Amagasaki, Hyogo 661-8661, Japan
Correspondence to: C. Feliciani (E-mail: claudio.feliciani@ce.mitsubishielectric.co.jp)

ABSTRACT: Recent improvements in injection molding numerical simulation software have led to the possibility of computing fiber orientation in fiber reinforced materials during and at the end of the injection molding process. However, mechanical, thermal, and electrical properties of fiber reinforced materials are still largely measured experimentally. While theoretical models that consider fiber orientation for the prediction of those properties exist, estimating them numerically has not yet been practical. In the present study, two different models are used to estimate the thermal conductivity of fiber reinforced thermoplastics (FRT) using fiber orientation obtained by injection molding numerical simulation software. Experimental data were obtained by measuring fiber orientation in injection molded samples' micrographs by image processing methods. The results were then compared with the numerically obtained prediction and good agreement between numerical and experimental fiber orientation was found. Thermal conductivity for the same samples was computed by applying two different FRT thermal conductivity models using numerically obtained fiber orientation. In the case of thermal conductivity, predicted results were consistent with experimental data measurements, showing the validity of the models. © 2013 Wiley Periodicals, Inc. J. Appl. Polym. Sci. **2014**, *131*, 39811.

KEYWORDS: fibers; thermal properties; thermoplastics; injection molding

Received 28 March 2013; accepted 2 August 2013
DOI: 10.1002/app.39811

INTRODUCTION

The addition of glass, carbon, or metallic short cut fiber to polymeric material has shown having great improvements in mechanical, electrical, and thermal properties with respect to the continuous phase. One of the main advantages of this kind of composite material, apart from its mechanical properties, is the ease of production, its cost, and the possibility of being used in industry established technology. Because of the above reasons, short fiber reinforced materials are being increasingly used in industrial applications and their properties have been focus of various studies. Particular interest on polymer composite materials has been addressed because of the capability of short fiber to improve material properties when used in combination with recycled plastics.[1–3]

Performance of polymer composites is particularly related to parameters defining its microstructure, such as fiber aspect ratio, length, orientation, and size distribution. While the fiber aspect ratio and length, together with fiber amount, can be chosen when the material mixture is created, orientation and size distribution strongly depend on manufacturing conditions and characteristics of both short fibers and the polymer matrix.

Among various industrial techniques for the production of polymer parts, injection molding is one of the most used techniques. High precision, possibility of large scale production, and the less time required to produce a single product are its biggest advantages. In injection molding, thermoplastics are heated above their flow temperature and are injected at high pressure inside mold cavities. If short fibers are added, their orientation will follow flow patterns during the injection phase. Fibers will maintain the orientation they had in the plastic flow phase matrix just before freezing. As a consequence, the study of the flow during injection plays an important role in the determination of fiber orientation, which is thus dependent on processing and geometrical parameters during the whole injection molding process. Remarkable parameters are cavity geometry, distribution of temperature and pressure inside the cavity, and rheological behavior of fiber suspension.

Since physical properties of fibers are much higher than the ones of the matrix (especially concerning electrical and thermal conductivity), fiber anisotropy plays an important role in estimating local physical properties of composite materials.

Recent development in commercial injection molding numerical software (such as Autodesk Moldflow Insight and TIMON)

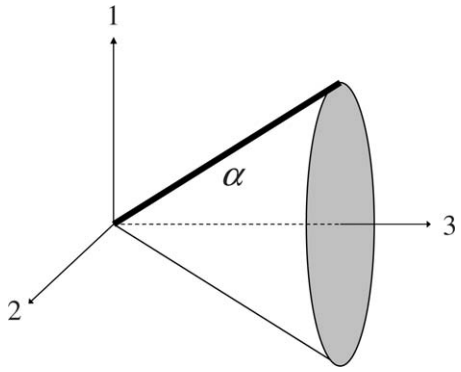

Figure 1. Angle formed from a fiber with 3-axis.

made them capable of computing flow patterns during the injection process, consequently predicting fiber orientation inside the final molded part. Accuracy of numerical prediction has been already the focus of various studies[4–7] and in general good agreement has been found with experimental results, thus confirming numerical methods as a successful way to predict fiber orientation.

This study proposes to use the fiber orientation computed with commercial injection molding software to predict thermal conductivity of fiber reinforced thermoplastics using composite thermal conductivity models from the literature. Comparison of the fiber orientation obtained numerically with experimental results, as well as comparison of predicted and measured thermal conductivity values will be provided to verify validity of the applied models.

THEORY

Expression of the Fiber Orientation

Numerical software is able to compute fiber orientation during injection molding using literature established models. Autodesk Moldflow Insight, used in this study for injection molding numerical simulation, makes use of the Folgan–Tucker[8] model, later extended to tensor notation by Tucker and Advani.[9] According to the model, the second order orientation tensor can be written as

$$a_{ij}=\begin{bmatrix} a_{11} & a_{12} & a_{13} \\ a_{21} & a_{22} & a_{23} \\ a_{31} & a_{32} & a_{33} \end{bmatrix} \tag{1}$$

where the suffixes of the tensor term express the three main spatial directions (see Figure 1 for reference). The original nine components reduce to five components due to tensor symmetry ($a_{ij} = a_{ji}$) and a normalization condition ($a_{11} + a_{22} + a_{33} = 1$). The three main components (a_{11}, a_{22}, and a_{33}) are a measure of the angle formed by one fiber with the corresponding axis. Considering Figure 1, the angle α formed by the represented black fiber with the 3-axis can be computed using the following equation

$$a_{33}=\cos^2\alpha \tag{2}$$

In a similar, the way angle formed by the same fiber with the 1- and 2-axes can be easily computed. It must be considered that, although a_{11}, a_{22}, and a_{33} offer a full description of the orientation with respect to the main spatial directions, because of their positive nature, they are not sufficient for a unique description of fiber orientation in a three dimensional space. Therefore, eigenvalues and eigenvectors of the fiber orientation tensor need to be computed.

However, the goal of this study being computation of thermal conductivity, only orientation relative to each axis is required as will be shown later on.

Fiber Length and Orientation Distribution

Because of the fiber alignment to flow patterns during injection molding, fiber orientation in the final mold part will result in a fiber distribution, which can be expressed using the fiber orientation distribution (FOD) density function given by[10–15]

$$g(\theta)=\frac{\lambda\, e^{-\lambda\theta}}{1-e^{-\lambda\pi/2}} \tag{3}$$

In this equation, λ is a parameter characterizing the degree of fiber orientation, its value being generally obtained by fitting with experimental data, which is preferably performed using the most easily fitted cumulative function. FOD cumulative function can be obtained by integrating FOD density function over the whole domain of θ obtaining the following expression

$$G(\theta)=\frac{1-e^{-\lambda\theta}}{1-e^{-\lambda\pi/2}} \tag{4}$$

The interaction of short fiber with wall and moving parts in the injection molding machine leads to a reduction of the unprocessed original fiber length. The length of the fibers inside the mold part will consequently not be constant and need to be expressed using a distribution function similarly as for fiber orientation. The fiber length distribution (FLD) density function can be given as[16]

$$f(L)=a\,b\,L^{b-1}\exp\left(-a\,L^{b}\right) \tag{5}$$

where a and b are respectively size and shape parameters, determining the size and shape of FLD curves. a and b can be obtained by fitting experimental data preferably with the cumulative FLD function obtained after integration of $f(L)$ over all possible length. Cumulative FLD function is given by

$$F(L)=1-\exp\left(-a\,L^{b}\right) \tag{6}$$

Generally speaking, if short fibers are employed, length reduction in the injection molding machine is reduced compared to the case of long fibers.[17] As a result, in the case of short fiber, a narrow fiber length distribution will be observed. The average fiber length therefore characterizes short fibers with good accuracy. As such, FLD plays a less important role compared to FOD and expressing fiber length with an experimentally obtained mean value may be sufficient.

At present, numerical injection molding software is unable to estimate the reduction of fiber length due to processing conditions, but, as stated before, if short fibers are employed, the use of an average value would be sufficient.

Fiber Composite Thermal Conductivity

Thermal conductivity equations for two-phase composites can be derived from Halpin–Tsai equation as shown by Nielsen[18]

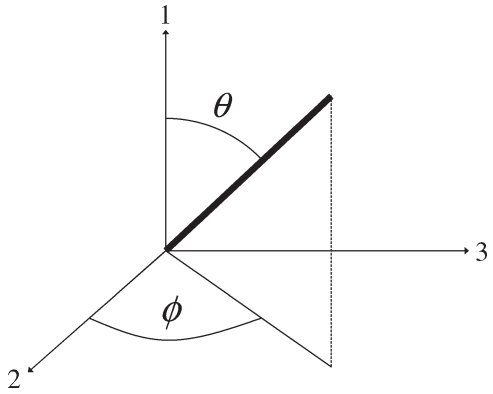

Figure 2. Fiber orientation in a three dimensional space.

and others.[19,20] By using laminate theory, thermal conductivity for a laminate composite may be obtained by considering a stacked sequence of laminae each with same fiber length and orientation.

Given matrix fiber parallel and transverse thermal conductivities (respectively K_m, K_{f1}, and K_{f2}) for a unidirectional composite lamina, thermal conductivities parallel (K_1) and perpendicular (K_2) to fiber direction can be expressed respectively as

$$K_1 = \frac{1+2\,\alpha\,\mu_1\,v_f}{1-\mu_1\,v_f}\,K_m \tag{7}$$

$$K_2 = \frac{1+0.5\,\mu_2\,v_f}{1-\mu_2\,v_f}\,K_m \tag{8}$$

where $\alpha = l/d$ is the aspect ratio, v_f the fiber volume fraction and μ_1 and μ_2 are given by

$$\mu_1 = \frac{(K_{f1}/K_m)-1}{(K_{f1}/K_m)+2\,\alpha} \tag{9}$$

$$\mu_2 = \frac{(K_{f2}/K_m)-1}{(K_{f2}/K_m)+0.5} \tag{10}$$

For a fiber oriented at an angle θ relative to the 1-axis of the lamina (see Figure 2), the thermal conductivities parallel to 1- and 2-axis are given by

$$K'_1 = K_1\cos^2\theta + K_2\sin^2\theta \tag{11}$$

$$K'_2 = K_1\sin^2\theta + K_2\cos^2\theta \tag{12}$$

If FLD and FOD are known, integration over all laminae leads to the expression for the thermal conductivity over the laminate parallel to the i-axis, given by[21]

$$K_{c,i} = \int_{L_{\min}}^{L_{\max}} \int_{\theta_{\min}}^{\theta_{\max}} K'_i\, f(l)\, g(\theta)\, dL\, d\theta \tag{13}$$

If FLD is unknown (and thus length integral in eq. (13) can be neglected) and FOD density function of eq. (3) is used, laminate thermal conductivities in directions 1 and 2 can be expressed as[22]

$$K_{c,1} = \frac{1}{2}(K_1+K_2) + \frac{1}{2}V_1(K_1-K_2) \tag{14}$$

$$K_{c,2} = \frac{1}{2}(K_1+K_2) - \frac{1}{2}V_1(K_1-K_2) \tag{15}$$

where

$$V_1 = \frac{\lambda^2\,(1+e^{-\lambda\pi/2})}{(\lambda^2+4)\,(1-e^{-\lambda\pi/2})} \tag{16}$$

The value of V_1 can be seen as a measure of fiber order, varying from 0 for random orientation to 1 for full alignment.

Fiber interaction can be included by using the method proposed by Fu and Mai.[21] In a first step only a small amount of fiber is inserted into the polymer matrix, this amount corresponding to the effective volume fraction given by

$$\mathrm{EV}_f = \frac{V_f}{2-V_f} \tag{17}$$

The obtained thermal conductivity will be used as matrix thermal conductivity in a second calculation, performed by adding the remaining amount of fiber (corresponding to a volume fraction of $\frac{1}{2}V_f$) to the partially filled composite obtained in the previous step (now considered as matrix). The interaction between short fibers can be realized in a manner such that the second half of fiber is incorporated into a previously fiber filled matrix material.

PREVIOUS STUDIES

Dependency between fiber orientation and composite thermal properties has been investigated by various authors in the past, although fiber orientation was always obtained by experimental methods.

Choy et al.[22] investigated various fiber reinforced thermoplastics (FRT) and compared theoretical results with experimental data. Their model was based on eqs. (14) and (15), where the fiber orientation parameter λ has been computed by fitting experimental fiber orientation obtained by analyzing polarizing microscope images. In their study, Choy et al. used polyphenylene sulfide (PPS) as matrix material in which carbon and glass fibers were included in a volumetric content varying from 30 to 40%. They computed thermal conductivity for the surface and middle layer. Experimental measurements for both layers confirmed the validity of the model used. A similar study from the same authors[23] used polyether ether ketone (PEEK) as matrix material combined with glass and carbon short fibers. Again laminate theory was confirmed being an adequate model to predict thermal conductivity in polymer composite materials.

Fu and Mai[21] extended the Choy et al. study by including FLD, thus making use of eq. (13) to model thermal conductivity. In addition, they considered fiber interaction (not included in the study of Choy et al.) in a two-step manner as described in the previous section. Fu and Mai based their experimental data for both fiber orientation and thermal conductivity on previously available values from literature. Their new model, applied to older fiber orientation data, increased thermal conductivity values (as a consequence of consideration of fiber interaction) thus finding an even better agreement compared with the study of Choy et al.

EXPERIMENTAL AND METHODOLOGY

Sample Preparation and Characteristics

Square plate samples with an edge length of 100 mm and a thickness of 2 mm were produced using an injection molding

Table I. Injection Molding Machine Settings

Regime maximum temperature	265°C
Mold temperature	60°C
Injection rate	30 mm/s
Holding pressure	70 MPa
Cooling time	20 s

machine manufactured by Nissei Plastic Industrial Co. Thermoplastic composite material Reny 1022F manufactured by Mitsubishi Engineering Plastics was used to produce the plate samples. Details on the setup of the injection molding machine and information regarding the material used are given in Tables I and II, respectively.

Reny 1022F composite material consists of polyamide (PA) matrix material reinforced with short glass fiber in an amount of 50% in weight (corresponding to a volume fraction of 32.2%). Materials properties and details for both PA matrix and glass fiber are given in Table III.

Fiber length and diameter undergo changes during the injection process[17] and a distribution of both quantities is usually observed in samples. In this study, however, average values were used to comply with the fact that numerical software used for the simulation of the injection molding process doesn't allow for an estimation of fiber length and diameter reduction. Fiber average diameter and length were, respectively, 11 μm and 200 μm.

From the main sample, smaller square subsamples with an edge length of 10 mm have been cut to be later used for thermal conductivity measurements. Position of subsamples has been chosen after analyzing mold flow patterns obtained by numerical simulations. Position chosen for subsamples and flow patterns are given in Figure 3.

Fiber Orientation Measurement

For the comparison of numerical fiber orientation with experimental data, a sample has been cut in the center, parallel to the 2-direction, and its cross-section has been analyzed in the central part (at the center of position A, as indicated in Figure 3). Three micrographs were taken (upper, lower, and central layer)

Table II. Composite Material Properties and Information

Composite type and manufacturer	
Family name	Polyamides (Polyamide MXD6)
Material structure	Crystalline
Trade name	Reny 1022F
Manufacturer	Mitsubishi Engineering Plastics
Fiber/filler	50% (mass fraction) glass fiber filled
Recommended processing settings	
Mold temperature	70–110°C
Melt temperature	240–300°C

Table III. PA Matrix and Glass Fiber Physical Properties

	Density	Heat capacity
Glass fiber	2.540 g/cm^3	0.700 J/g K
PA matrix	1.204 g/cm^3	1.349 J/g K
Composite	1.634 g/cm^3	1.024 J/g K

and combined to obtain a single image describing fiber orientation in the 1–2 plane. Images of sample cut are given in Figure 4. The micrograph shows some basic features related to the processing techniques and the materials used. In first instance, it is possible to notice that most of the fibers oriented parallel to the cutting plane have a length close to 200 μm, showing that length reduction during injection molding was not pronounced. In addition, the large number of circles in the central part of the image identifies the region of the main resin flow. By considering that the resin is flowing from the right to the left side of the figure, it is possible to conclude that resin will first flow in the central part of the sample and only later fill the lower and upper part of the mold cavity, where the fibers are oriented parallel to the cross-section.

Fiber orientation has been obtained from micrographs using the commercial image processing software IGOR. Fiber detection has been made possible by classical image processing operations such as thresholding and object detection. Fiber angle measurement has been performed by analyzing elliptical shapes formed by cut fibers[5,24–27] easily recognizable in Figure 4.

Experimental fiber orientation can be computed by considering the fact that, from a geometrical point of view, the intersection of a plane and a cylinder of infinite length with any given angle between them will result in an elliptical shape. A circle (which can

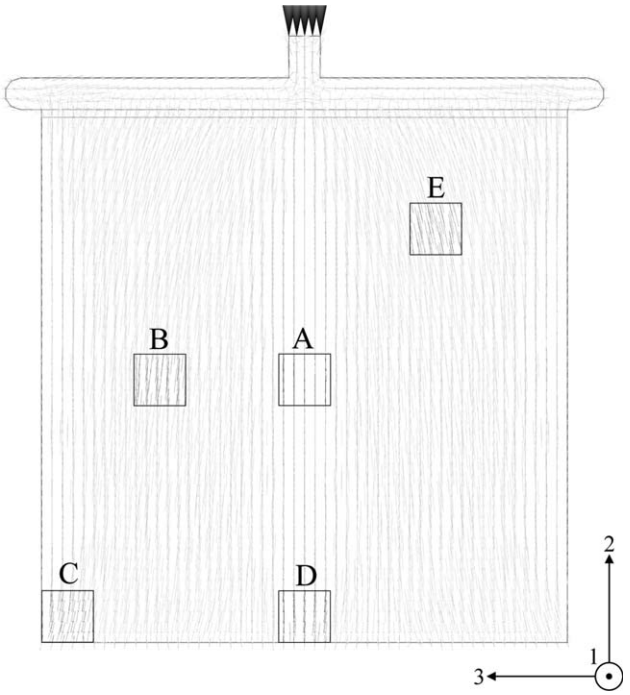

Figure 3. Subsamples position and orientation.

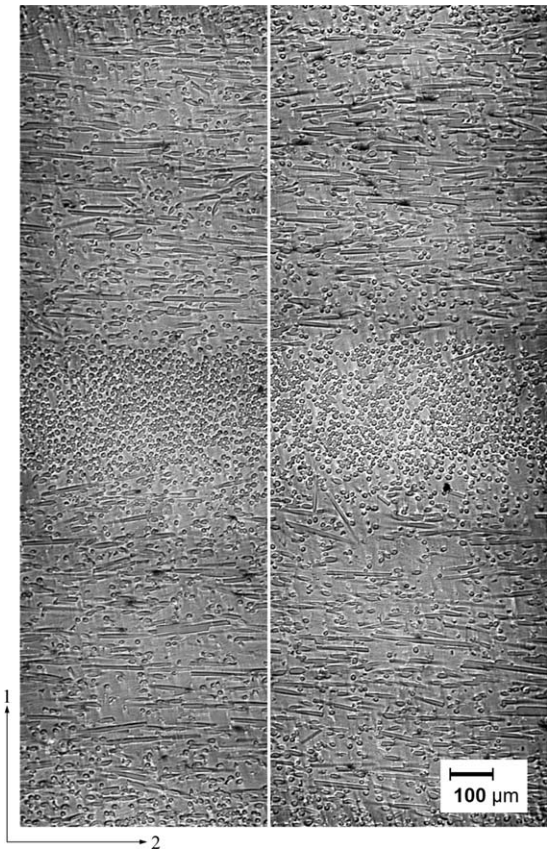

Figure 4. Micrograph of sample cut representing 1–2 plane. Fibers are clearly visible as dark ellipses.

be considered as a particular ellipse) will be obtained in cases where the intersecting plane is perpendicular to the cylinder's axis, and an ellipse of infinite length will be obtained in cases where the intersecting plane is parallel to the cylinder's axis.

In cutting the sample, the exposed cross-section shows the intersection of the cylindrical fibers, as represented by the above scenario. They are therefore observed as elliptical shapes in the micrograph (as illustrated in Figure 5) and angle θ in the 1–2 plane can be easily computed by measuring the angle formed

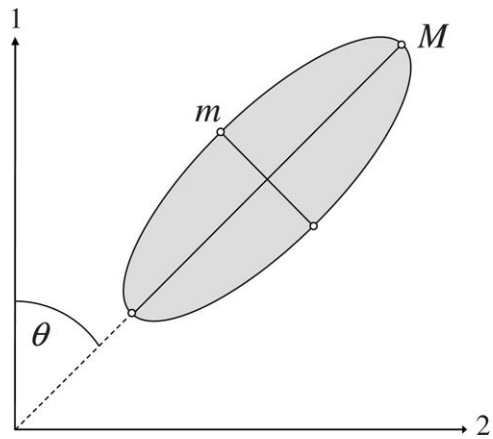

Figure 5. Elliptical shape of fiber cut in micrograph and geometrical interpretation.

with 1-axis from the ellipse major axis M. Angle ϕ can be obtained by measuring ellipse major axis M and minor axis m and applying following equation

$$\sin\phi = \frac{m}{M} \tag{18}$$

For each image about 4000 fibers were detected and their three dimensional orientation (angle θ and ϕ) successfully measured.

Method for the Estimation of Numerically Obtained Thermal Conductivity

Prediction of subsamples thermal conductivity is made by exporting fiber orientation tensor obtained after injection molding simulation with Autodesk Moldflow Insight. The finite element model used for the simulation comprised 447,428 tetrahedral elements, each element containing an orientation tensor describing the orientation of the fiber in its corresponding position inside the model. For the calculation of subsamples thermal conductivity only the elements contained in the subsamples area are relevant. Consequently as a first step, elements in position corresponding to subsamples area were extracted thus reducing the number of the elements used for the thermal conductivity prediction to about 10,000. Once relevant elements were extracted, angle for each fiber (element) with the 1-axis (direction of thermal conduction for experimental comparison) has been computed. From these angles, FOD density function could be computed.

Afterwards, two different methods have been used for the computation of thermal conductivity. In the direct computation method, eq. (13) has been used directly to obtain subsample thermal conductivity. In the second method, FOD cumulative function has been first computed to fit data obtained with theoretical curve of eq. (4). From that fitting, λ fiber orientation factor has been obtained and successively used for the computation of thermal conductivity in 1-direction according to eqs. (14) and (16).

The method used for thermal conductivity calculation from simulation data is schematically represented in Figure 6.

Thermal Conductivity Measurements

Experimental subsample's thermal conductivity in 1-direction ($K_{c,1}$) has been obtained after measuring thermal diffusivity (α), density (ρ), and heat capacity (c_p) and multiplying the three terms according to the following equation

$$K_{c,1} = \alpha\, c_p\, \rho \tag{19}$$

Thermal diffusivity measurements were performed using a NETZSCH LFA 447 NanoFlash Xenon Flash Apparatus. In this device, subsamples are shot on their lower side using a Xe flash lamp and its thermal diffusivity is obtained by analyzing the immediate temperature rise on the opposite side. For each subsample, thermal diffusivity has been obtained by averaging the results of four light pulses.

Heat capacity has been measured using an EXSTAR DSC6220 differential scanning calorimeter manufactured by SII Nano-Technology. In DSC devices, sample and a reference material (sapphire has been used for this study's measurements) are

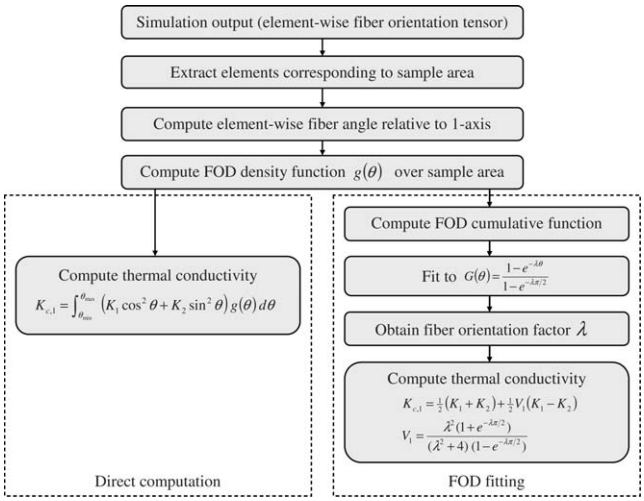

Figure 6. Schematic representation of the method used for predicting composite thermal conductivity from numerical simulation data.

equally raised in temperature (in this study from 0 to 100°C at a heating rate of 10°C/min) and differential heat required to maintain them at the same temperature is measured. Heat capacity over the temperature range can then be computed from differential data. DSC measurements were performed in a nitrogen atmosphere using samples with an average weight of 10 mg.

Finally, density has been measured by means of a digital densimeter (Mirage ED-120T electronic densimeter). In all cases, values have been chosen for a temperature of 25°C. Relative accuracy for thermal conductivity measurements lies at about 3%.

A virgin PA sample (consisting only of PA matrix material) has been produced and thermal diffusivity, heat capacity, and density have been measured using the above described experimental equipment. Thermal conductivity for PA matrix was found to be 0.271 W/m K (corresponding experimental value for thermal diffusivity was of 0.167 mm^2/s). Fiber's thermal conductivity was given by the manufacturer as 1.000 W/m K.

Because of their isotropic character, heat capacity and density of the composite material could be obtained by combining matrix and fiber raw material properties considering mass (50%) and volume fraction (32.2%) respectively. However, thermal diffusivity is largely anisotropic in composite materials; therefore this was experimentally measured on subsamples.

RESULTS AND DISCUSSION

Comparison Between Experimental and Numerically Simulated Fiber Orientation

Comparison between experimental and numerical fiber orientation has been performed by calculating fiber orientation in 1–2 and 2–3 plane from micrographs (see Figure 4) and comparing the data obtained with the ones of numerical simulation.

Figure 7 shows numerical and experimental fiber orientation for the central section of the composite sample in the 1–2 plane (angle θ). Numerical fiber orientation is given in black, while

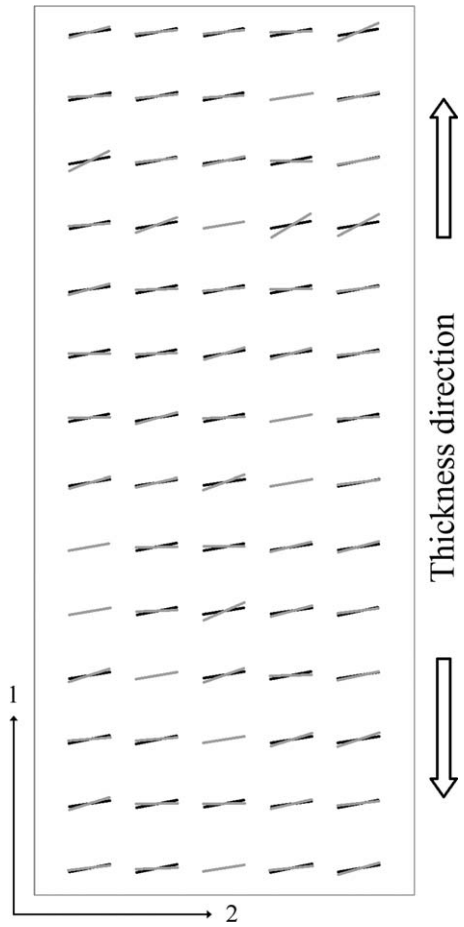

Figure 7. Comparison between experimental (gray) and numerical (black) fiber orientation (θ-angle) in the sample central position.

experimental data for the same position is given in gray. In general, good agreement with experimental data can be found, although experimental data shows more random behavior. This difference can be explained by considering that numerical software is not able to compute fiber–fiber interactions during injection phase. In addition, wall interaction and inhomogeneities during the whole process (slightly different cooling rate depending on location, not homogeneous fiber–matrix mixture) may lead to differences between experimental and numerical results.

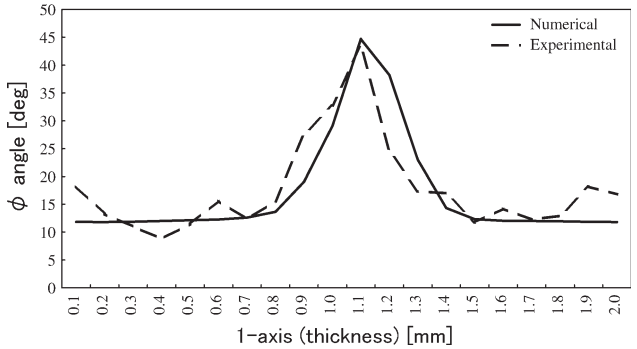

Figure 8. Comparison between experimental (dashed line) and numerical (solid line) fiber orientation (ϕ-angle) in the sample central position.

Table IV. Comparison Between Experimental and Numerical Thermal Conductivity in Different Locations

	Thermal conductivity [W/m K]				
Location	A	B	C	D	E
Experimental	0.389	0.371	0.405	0.424	0.397
Numerical—direct method	0.383	0.384	0.394	0.391	0.384
Deviation	−1.6%	+3.4%	−2.8%	−8.4%	−3.4%
Numerical—FOD fitting	0.393	0.394	0.404	0.400	0.394
Deviation	1.0%	5.8%	−0.2%	−6.0%	−0.8%

In Figure 8 the angle ϕ formed by fiber with the 2-axis in the 2–3 plane is visualized along the thickness of the sample. Angle ϕ can be seen as the out-of-plane angle formed by fiber in the 1–2 plane of Figure 7. Again good agreement with experimental data can be found, with the top of the central peak being almost the same for both data sets. The biggest difference can be found in the upper and lower section (at a thickness of 0.1 and 2.0 mm respectively). This difference can be explained by considering that numerical software are unable to compute wall–fiber interactions.

In general, good agreement between experimental and numerical data has been found for both θ- and ϕ-angle. Only close to the wall boundary some discrepancy between both data sets has been observed, which may become a problem when the production of very thin parts need to be simulated. However, being this difference only limited to the very close boundary, it can be concluded that numerically obtained fiber orientation can be used for the study of anisotropic physical properties of composite materials.

Thermal Conductivity

The thermal conductivity computed in five different locations (see Figure 3) with both direct method and FOD fitting method and their corresponding experimental values are given in Table IV.

In general, good agreement between experimental and numerical thermal conductivity can be found, with the FOD fitting method performing at best. The accuracy in the prediction of fiber orientation plays a major role here, as a composite with random oriented fibers (thus the V_1-value of eq. (16) is equal to zero) would lead to a thermal conductivity of 0.435 W/m K; clearly higher than the experimentally measured value.

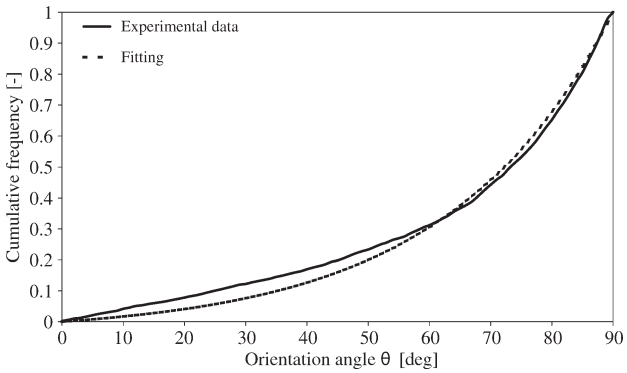

Figure 9. FOD cumulative function for the orientation angle θ in sample central position. Experimental data and fitting with theoretical function.

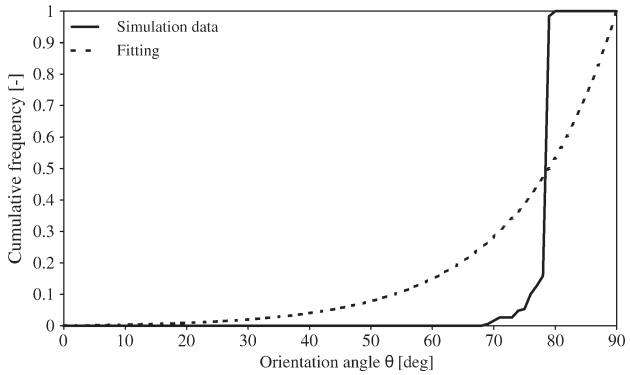

Figure 10. FOD cumulative function for the orientation angle θ in sample central position. Numerical data and fitting with theoretical function.

However, as for the fiber orientation, experimental data for thermal conductivity shows larger variation depending on location than numerical data. Again this behavior can be explained by considering that imperfections and various phenomena appearing in reality cannot be simulated in a numerical way.

In order to understand the reason why FOD fitting method gives better results than direct method some further investigation has been done. For subsample A (corresponding to the center's sample), FOD cumulative function for the angle θ (thus the angle in thermal conductivity direction) has been computed from both experimental data (obtained from micrographs) and numerical data. In both cases, the curve has been fitted with theoretical function [eq. (4)]. The results are given in Figures 9 and 10.

The experimental curve increase steadily until about 60° (with a cumulative amount of 30%), after which the curve increases faster. This means that most of the fibers have an orientation higher than 60° and thus are mostly perpendicular to the direction of thermal conduction. Although performing only scarcely in the lowest region, the fitting is able to describe data with sufficient accuracy. On the other hand, numerical FOD cumulative curve show a step-wise behavior, being invalid until about 70° and becoming accurate at about 80°. According to simulation data, fibers with an orientation smaller than about 70° should not be found.

Again, the lack of a fiber–fiber interaction model in the simulation is one of the main causes explaining the discrepancy between both curves, but other parameters contribute as well. In this context, it has to be reminded that numerical simulations reproduce ideal conditions, which are usually not found in reality.

In particular, the temperature of the mold cavity and physical properties of the composite at the time of its injection are considered homogenous in simulation. In reality, even by using modern injection molding equipment, mold temperature shows cold and hot regions, which leads to numerically unpredictable

Table V. Thermal Conductivity of Different Composites in the Study by Fu and Mai (Thermal Conductivity of PEEK Matrix is 0.243 W/m K and Longitudinal Thermal Conductivity of the Carbon Fiber is 9.4 W/m K in the case of PPS and 8.0 W/m K in the Case of PEEK)

Material				Thermal conductivity [W/m K]	
Matrix	Fiber	Volume fraction	Layer	Experimental	Theoretical
PPS	Glass	26.4%	Surface	4.08	3.96
			Middle	3.99	3.89
PPS	Carbon	33.5%	Surface	17.2	19.76
			Middle	15.6	16.96
PPS	Carbon	24.3%	Surface	15.2	14.96
			Middle	12.4	12.88
PEEK	Carbon	21.4%	Surface	11.6	11.87
			Middle	10.8	11.16

effects concerning fiber motion inside the resin mold. In addition to temperature effects, deviations from theoretical models used for computing viscosity and *pVT*-properties during simulations are some of the causes which can lead to a more random distribution of the fibers found in experimental data.

Finally, an average fiber length has been used instead of the fiber length distribution found in reality. Although this approximation is satisfactory for the aim of this study, a distribution should be used to improve accuracy of the simulation's results, leading to a smoother curve for fiber orientation. However, this possibility is currently excluded because of limitations of simulation software.

During injecting, most of the fiber will be orient in the flow direction, but, because of various fiber interactions, a small part will deviate leading to the smooth experimental curve. On the other hand, simulation software assumes that fibers will orient exactly according to flow lines thus creating the step wise curve show in Figure 10.

Although both curves look very different, when fitting is performed, similar values for λ are obtained. By comparing dashed line curve of Figure 10 (fitting of numerical data) with solid line of Figure 9 (experimental data) the difference is minimal.

As a consequence of these observations FOD fitting method, because of its capability to reproduce in a greater accuracy FOD function, will perform better in thermal conductivity calculations. On the other side, direct method, although using stepwise FOD function, obtained results in good agreement with experimental, demonstrating that, since thermal conductivity is computed by integral way, only the area under the FOD curve plays an important role, not its shape.

Comparison with Previous Studies

Results obtained in this study are in line with previous research from the literature. In particular, a comparison with the results by Fu and Mai[21] shows that, if accurate fiber orientation data are provided, thermal conductivity can be estimated with good agreement.

Fu and Mai investigated thermal conductivity in different composite materials. Among the composites used in their study, there is a glass fiber reinforced PPS composite having thermal properties close to the constituent materials chosen in the present study. In the research by Fu and Mai, thermal conductivity values for the PPS matrix and glass fibers were, respectively, 0.2 W/m K and 1.04 W/m K. Fiber content volume fraction was comparable to the value used here, being, in their case, 26.4%. The authors based their predictions on experimentally measured fiber orientation obtained by examining enlarged microscope images. Their results for the theoretical and experimental thermal conductivity in the middle and surface layer across the thickness of the sample are reported in Table V. As the table shows, a relatively good agreement with experimental data for all the investigated composites is found, concluding that the modified Halpin–Tsai thermal conductivity equations can be successfully used to estimate thermal conductivity in a range of composite materials.

With the present research, we demonstrated that accurate prediction for thermal conductivity in FRT can be done in a purely numerical way, without having to rely on experimental methods to examine fiber orientation in an intermediate step.

CONCLUSIONS

A procedure for the computation of composite thermal conductivity by means of numerical simulation has been proposed. On the scope two different methods have been used: direct computation and FOD fitting. The second method has shown obtaining better agreement with experimental data, because of its capability to compute FOD functions with better accuracy.

Fiber orientation obtained numerically has shown being in good agreement with experimental results, both concerning angle ϕ and θ.

Similarly good agreement has been found for thermal conductivity values with an average deviation of 2.6% from experimental data (FOD method). The results obtained show that the method proposed in this study, based on fiber orientation, can be successfully applied for thermal analysis in composite materials.

However, it is important to remark that, although fiber orientation plays a major role in determining thermal conduction of fiber reinforced composites, other parameters such as aspect ratio, connectivity of the fiber, adhesion of the fiber and the matrix, fiber packing behavior, and porosity of the composite should be considered to further improve prediction capabilities and accuracy of the method, finally obtaining a more random behavior as observed in experimental data.

In particular, as several studies showed,[21–23,28] fiber aspect ratio plays a significant role in determining thermal properties of composite materials. In the case of injection molding, where fiber length and diameter change inside the molding machine, local values of fiber aspect ratio inside the sample/product should be included when computing thermal conductivity. In a

similar way to the approach used here for fiber orientation, fiber aspect ratio could be accounted as a distribution inside a given region to further increase prediction accuracy. However, as numerical simulation software currently only allows estimation of the fiber orientation, experimental values should be used for local fiber aspect ratio, making the prediction a hybrid combination of experimental and numerical method. In the future, with the evolution of simulation software, an extension of the present model, including local aspect ratio, can be considered. In a later step, with numerical models and software making additional improvements, an increasing number of phenomena (local porosity, local connectivity, …) could be accounted for, further improving prediction accuracy.

FUTURE STUDIES

As listed in the conclusions, in line with the evolution of simulation software, future studies may include local variations of an increased number of parameters. In addition, the method described might be extended for unsteady thermal simulation involving heat conduction in multiple directions. On this behalf, element-wise fiber orientation can be used to compute corresponding three-dimensional thermal conductivity by direct method to be later used in finite element numerical software for thermal analysis.

REFERENCES

1. Chtoutou, H.; Riedl, B.; Ait-Kadi, A. *J. Reinf. Plast. Compos.* **1992**, *11*, 372.
2. Lei, Y.; Wu, Q.; Yao, F.; Xu, Y. *Compos. A* **2007**, *38*, 1664.
3. Muzzy, J. D.; Holty, D. W.; Eckman, D. C.; Stoll, J. R. *(Georgia Composites). U.S. Pat.* 6,271,270 B1 (**2001**).
4. Lee, K. S.; Lee, S. W.; Chung, K.; Kang, T. J.; Youn, J. R. *J. Appl. Polym. Sci.* **2003**, *88*, 500.
5. Kim, E. G.; Park, J. K.; Jo, S. H. *J. Mater. Process. Technol.* **2001**, *111*, 225.
6. Gupta, M.; Wang, K. K. *Polym. Compos.* **1993**, *114*, 367.
7. Tucker, C. L.; VerWeyst, B. E.; Foss, P. H.; O'Gara, J. F. *Int. Polym. Process.* **1999**, *14*, 409.
8. Folgar, F. P.; Tucker, C. L. *J. Reinf. Plast. Compos.* **1984**, *3*, 98.
9. Tucker, C. L.; Advani, S. G. *J. Rheol.* **1987**, *31*, 751.
10. Fu, S. Y.; Lauke, B. *Compos. Sci. Technol.* **1998**, *58*, 1961.
11. Lauke, B.; Fu, S. Y. *Compos. Sci. Technol.* **1999**, *59*, 699.
12. Fu, S. Y.; Lauke, B. *Compos. Sci. Technol.* **1998**, *58*, 389.
13. Fu, S. Y.; Hu, X.; Yue, C. Y. *Compos. Sci. Technol.* **1999**, *59*, 1533.
14. Fu, S. Y.; Lauke, B. *J. Mater. Sci.* **1993**, *32*, 1985.
15. Fu, S. Y.; Lauke, B. *Compos. Sci. Technol.* **1996**, *56*, 1179.
16. Fu, S. Y.; Yue, C. Y.; Hu, X.; Mai, Y. W. *J. Mater. Sci. Lett.* **2001**, *20*, 31.
17. Patcharaphun, S.; Opaskornkul, G.; Kasetsart J. *Nat. Sci.* **2008**, *42*, 392.
18. Nielsen, L. E. *Ind. Eng. Chem. Fundam.* **1974**, *13*, 17.
19. Bigg, D. M. *Polym. Compos.* **1986**, *7*, 125.
20. Progelhof, R. C.; Throne, J. L.; Ruetsch, R. R. *Polym. Eng. Sci.* **1976**, *16*, 615.
21. Fu, S. Y.; Mai, Y. W. *J. Appl. Polym. Sci.* **2003**, *88*, 1497.
22. Choy, C. L.; Leung, W. P.; Kowk, K. W.; Lau, F. P. *Polym. Compos.* **1992**, *13*, 69.
23. Choy, C. L.; Leung, W. P.; Kowk, K. W.; Lau, F. P. *J. Polym. Sci.* **1994**, *32*, 1389.
24. Lee, Y. H.; Lee, S. W.; Youn, J. R.; Chung, K.; Kang, T. *J. Mater. Res. Innovat.* **2002**, *6*, 65.
25. Gadala-Maria, F.; Parsi, F. *Polym. Compos.* **1993**, *14*, 126.
26. Jung, S. W.; Kim, S. Y.; Nam, H. W.; Han, K. S. *Compos. Sci. Technol.* **2001**, *61*, 107.
27. Kim, J. W.; Lee, D. G. *J. Mater. Process. Technol.* **2008**, *201*, 755.
28. Chen, C. H.; Wang, Y. C. *Mech. Mater.* **1996**, *23*, 217.